Research Papers

An Approach to Design Broadband Air Backed Piezoelectric Sensor

Mohamed G.S. ALI, Nour Z. ELSAYED, Ebtsam A. EID

Physics Department, Minia University
Egypt; e-mail: mgalal09@yahoo.com

In this work, an approach to the design of broadband thickness-mode piezoelectric transducer is presented. In this approach, simulation of discrete time model of the impulse response of matched and backed piezoelectric transducer is used to design high sensitivity, broad bandwidth, and short-duration impulse response transducers. The effect of matching the performance of transmitting and receiving air backed PZT-5A transducer working into water load is studied. The optimum acoustical characteristics of the quarter wavelength matching layers are determined by a compromise between sensitivity and pulse duration. The thickness of bonding layers is smaller than that of the quarter wavelength matching layers so that they do not change the resonance peak significantly. Our calculations show that the -3 dB air backed transducer bandwidth can be improved considerably by using quarter wavelength matching layers. The computer model developed in this work to predict the behavior of multilayer structures driven by a transient waveform agrees well with measured results. Furthermore, the advantage of this this model over other approaches is that the time signal for optimum set of matching layers can be predicted rapidly.

Keywords: piezoelectric, equivalent circuits, impulse response, frequency response, matching layers, z-transform.

1. Introduction

In ultrasonic broadband applications such as medical imaging or non-destructive testing piezoelectric transducers should generate/receive ultrasonic signals with good efficiency over a large frequency range. This requires the use of broadband piezoelectric transducer with high sensitivity and short-duration impulse response. Piezoelectric ceramic transducers usually have a specific acoustic impedance much greater than those of the usual load present in diagnostic ultrasound ones. This impedance difference generates ultrasonic pulses of pulse width much larger than electric signals. For reducing the multiple internal reflections, front impedance matching layers between piezoelectric transducer and load medium are required (BEERMAN, 1981; PERSSON *et al.*, 1985; TODA *et al.*, 2010). Several theoretical models for calculating the optimum acoustic impedance for the front matching layers are reported in the literature (SHUNG *et al.*, 2007; KAZYS *et al.*, 2006). The acoustic backing material is used at the back of the transducer for damping the free oscillation. However, these materials absorb acoustic energy and therefore reduce the transducer sensitivity (KONOVALOV, 2002). The effect of air backing on receiving sensitivity for piezoelectric micro-machined hydrophone was investigated (LEE *et al.*, 2010). MULHOLLAND *et al.* (2008) developed a linear system model for a composite piezoelectric transducer with multiple matching layers. The transmission line model is widely used for designing efficient broad band air backed piezoelectric transducers. The transmission line model is normally Fourier transform representation of the piezoelectric transducer and therefore yields solutions in terms of angular frequency. Researchers (DESILETS *et al.*, 1978; LEWIS, 1980; CHEN, 2010) typically use frequency domain equivalent circuits and derive the time domain transient response by inverse fast Fourier transform (FFT). The mathematical treatment is complicated when more than two layers are considered and the technique is restricted to certain excitations. Transformations of the transducer equivalent circuit in discrete time domain was described by (ESTANBOULI *et al.*, 2006) and (KAZYS *et al.*, 1977).

This work presents a more complete model for predicting the behavior of a multilayered piezoelectric transducer. It uses z-transform techniques to provide a discrete time implementation of the original fre-

quency domain circuit of Mason (BERLINCOURT *et al.*, 1964; KAZYS, 1978). The optimum acoustical characteristics of the matching layers are determined by defining a compromise between the sensitivity and the duration time of the impulse response. Also the effect of bonding layers on the resonance frequency of a transducer is studied.

2. Transducer equivalent circuits

Transducer performs the conversion of electrical energy into mechanical energy and vise verse (ALI *et al.*, 2012). There is a fundamental relationship between the properties of the transducer and the quality of the resulting image; a several techniques have been developed for modelling transducer behaviour and hence predicting the required system response. Many computer models that describe the behaviour of ultrasonic piezoelectric transducer are currently available (YAACOB *et al.*, 2011; SHERRITY *et al.*, 1997; TODA *et al.*, 2012). In this paper a simulation is applied using the developed computer model (ALI, 1999) to evaluate the discrete time response. The computer model is split into two parts. First, the basic transfer function of the loaded piezoelectric element is evaluated in discrete form using the Z-transform technique. Second, the discrete time responses obtained in that way are processed by a nested set of digital filter operations that simulate the reverberation in the coupling layers connected to the transducer and the backing and medium load.

The three required transfer functions of the transducer depicted in Fig. 1 are: a voltage transfer function relating the excitation voltage (V_s) to the voltage developed across the transducer terminals (V); a transmit transfer function relating the force generated (F_0) to a voltage excitation (V_s); and a receiver transfer function relating the force incident on the transducer front face (F_i) to the voltage developed across the transducer terminals (V). The basis for the development of the expression for the above transfer functions is a generalization of the circuit of Fig. 1. The generalized circuit depicted in Fig. 2 will allow the simple derivation of the transfer function. From this circuit particularly simple transfer functions and impedances can be expressed as described below:

$$\frac{V}{V_s} = \frac{sC_0 R_M - \phi^2}{sC_0[1 + sC_0 R_s]R_M - \phi^2}, \quad (1)$$

$$\frac{V_{RM}}{V_s} = \frac{sC_0 R_M}{sC_0[1 + sC_0 R_s]R_M - \phi^2}, \quad (2)$$

$$\frac{V}{V_M} = \frac{sC_0 R_M}{sC_0[1 + sC_0 R_s]Z_A - \phi^2}, \quad (3)$$

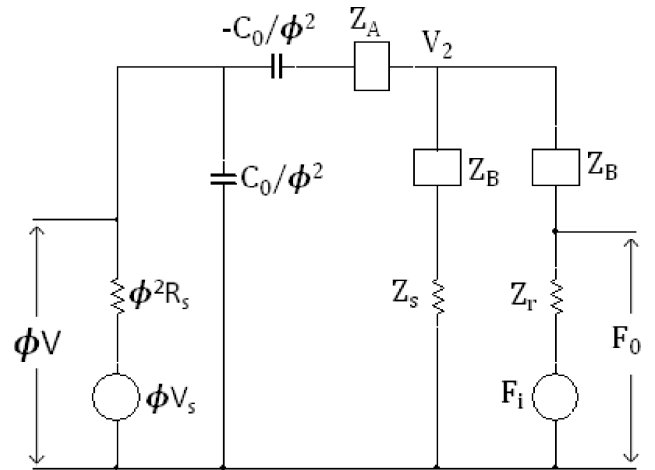$$R_s = \frac{sC_0[1 + sC_0 R_s]Z_A - \phi^2}{sC_0[1 + sC_0 R_s]Z_A}. \quad (4)$$

Fig. 1. Equivalent circuit of the piezoelectric transducer: V_s excitation voltage; C_0 static capacitance of the piezoelectric element; ϕ electrical to mechanical conversion factor; Z_A, Z_B distributed components of the familiar 'T' equivalent circuit of a transmission line; Z_r, Z_s acoustic impedance of the materials in contact with the front and back face of the piezoelectric element; F_0 transmitted force; F_i received force; and V voltage seen across the terminals of the transducer.
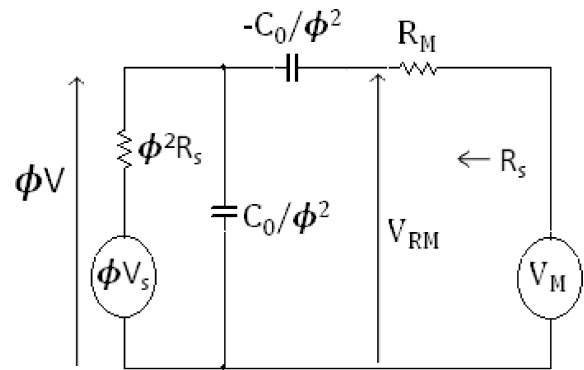

Fig. 2. Simplified general circuit. R_M represents two impedance.

For the case of no incident force on the face of the transducer, from Fig. 1, R_M is seen to be the impedance looking into center tapped transmission line terminated by distributing impedances Z_r and Z_s. This is shown in Fig. 3, from which it can be seen that:

$$R_m = \frac{2Z_A Z_B + Z_B^2 + (Z_A + Z_B)(Z_r + Z_s) + Z_r Z_s}{2Z_B + Z_r + Z_s}. \quad (5)$$

In Fig. 1 Z_A and Z_B represent the distributed components of the familiar T equivalent circuit of a transmission line. However, in this case Z_A and Z_B have a mechanical interpretation:

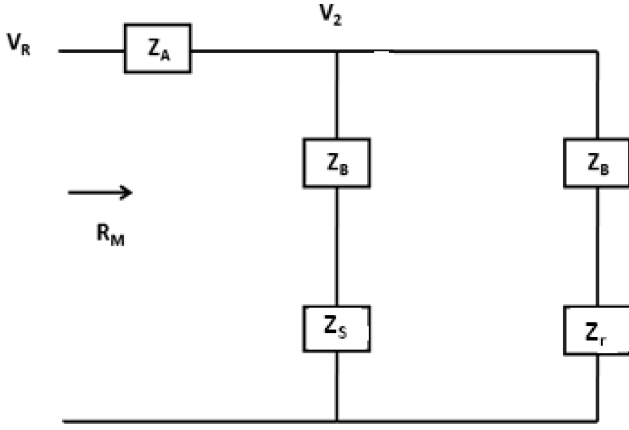$$Z_A = \frac{2Z_C}{e^{sX/V} - e^{-sX/V}} \quad (6)$$

Fig. 3. The equivalent circuit of the impedance R_M which is that looking into a center tapped transmission line terminated with impedance Z_r and Z_s.

and

$$Z_B = Z_C \frac{1 - e^{-sX/V}}{1 + e^{-sX/V}}, \qquad (7)$$

where Z_C is the acoustic impedance of the piezoelectric element and V is the velocity of compression waves in the piezoelectric material. The term $X/V = T_P$ represents the time delay for an acoustic wave to propagate from one face of the piezoelectric element to the other. It is clear that a number of discrete time intervals can approximately represent the time delay $T_P = m_0 T$, where m_0 is an integer and T is the sampling period. OPPENHEIM *et al.* (1975) and JURY (1964) discussed the properties of z-transform and its relationship to the Fourier and Laplace transform. In terms of the Laplace transform, the time delay $\exp(-sX/V)$ approximates to $\exp(-sm_0 T) = z^{-m_0}$, where the substitution $z = \exp(sT)$ has been made and the approximate time delay is given in terms of the z-transform. The impedance of R_M, Z_r, Z_s, and R_s can be presented as polynomial quotient expression:

$$R_M = \frac{R_{M\text{num}}}{R_{M\text{den}}}, \qquad Z_r = \frac{Z_{r\text{num}}}{Z_{r\text{den}}},$$
$$\qquad\qquad\qquad\qquad\qquad (8)$$
$$Z_s = \frac{Z_{s\text{num}}}{Z_{s\text{den}}}, \qquad R_s = \frac{R_{s\text{num}}}{R_{s\text{den}}}.$$

2.1. The voltage response (voltage-voltage)

Substituting the above expression into Eq. (1) produces the full expression for the voltage transfer function:

$$V = \frac{V_s R_{s\text{den}}[sC_0 R_{M\text{num}} - \phi^2 R_{M\text{den}}]}{sC_0[R_{s\text{den}} + sC_0 R_{s\text{num}}]R_{M\text{num}} - \phi^2 R_{M\text{den}}}. \quad (9)$$

2.2. The transmit response (voltage-force)

The calculation of transmission and reception transfer functions involves a two-step procedure. For the transmit response, first the response at the point labeled V_2 in Figs. 1 and 3 is obtained. Next the transmitted force across the matching layers is calculated from the response at V_2. From Fig. 3 it can be deduced that

$$10V_s = \frac{[Z_B^2 + Z_B(Z_r + Z_s) + Z_r Z_s]V_{RM}}{a^*} \quad (10)$$

where

$$a^* = 2Z_A Z_B + Z_B^2 + (Z_A + Z_B)(Z_{RF} + Z_{RB}) + Z_{RF} Z_{RB},$$

where Z_{RB} and Z_{RF} are terminating impedances at the back and front of the transducer assembly respectively, that is the material of infinite length. From Eq. (2), Eq. (10) becomes

$$V_2 = \frac{s\phi C_0[Z_B^2 + Z_B(Z_r + Z_s) + Z_r Z_s]V_s}{b^*}, \quad (11)$$

where

$$b^* = sC_0[1 + sC_0 R_s][2Z_A Z_B + Z_B^2$$
$$+ (Z_A Z_B)(Z_r + Z_s) + Z_r Z_s] - \phi^2[2Z_B + Z_r + Z_s].$$

In this work, using four matching layers and the transfer of force through these layers (ALI, 1999) from piezoelectric element of impedance Z_c to an impedance Z_r, the final expression for the transmit response can be obtained by substituting Eqs. (6) and (7) into Eq. (11) and rearranging. It can be shown that:

$$F_0 = \frac{c^*}{2[1 + Ar_0 z^{-m_0} + (r_0 + z^{-m_0} B)]}, \quad (12)$$

where

$$c^* = V_2[1 + (1 + r_1)(1 + r_2)(1 + r_3)$$
$$\cdot (1 + r_4)z^{-(m_0 + m_1 + m_2 + m_3 + m_4)}],$$

where A and B are functions of the reflection coefficients (r_0, r_1, r_2, r_3, r_4) referring to the interface between the layers; m_0, m_1, m_2, m_3, m_4 integer numbers (ALI, 1999).

2.3. The receiver response (force-voltage)

Upon reception, the force transfer across an arbitrary number of matching layers has to be calculated. This involves the impedance of far side of the last layer being that of the impedance looking into the transducer from the front face of the piezoelectric element, Z_{eq} as shown in Fig. 1. From Fig. 1 and Eq. (4) Z_{eq} can be written as:

$$Z_{eq} = \frac{d^*}{sC_0[1 + sC_0 R_s][Z_A Z_B + Z_s] - \phi^2}, \quad (13)$$

where

$$d^* = sC_0[1 + sC_0 R_s][2Z_a Z_B + Z_B^2 + Z_s[Z_A + Z_B]]$$
$$- \phi^2[Z_s + 2Z_B].$$

Substituting Eqs. (6) and (7) into Eq. (13) and quotient form of Z_s and may be written as:

$$Z_{eq} = \frac{Z_{eqnum}}{Z_{eqden}}. \tag{14}$$

With the reflection coefficients arranged to calculate force transfer in the opposite direction to that defined previously and the last reflection coefficient for the fourth matching layer, r_4 is defined as $r_4 = (Z_{eq} + Z_1)/(Z_{eq} - Z_1)$. The response in terms of the incident force F_i can be calculated as:

$$F_i = \frac{e^*}{a(A + r_0 B)}, \tag{15}$$

where

$$e^* = 2F_i Z_{eqnum}(1 + r_0)(1 + r_1)$$

$$\cdot (1 + r_2)(1 + r_3)z^{-(m_1 + m_2 + m_3 + m_4)}.$$

From Fig. 1. and Fig. 2. a simplified circuit can be used to obtain the voltage V_M, as shown in Fig. 4, as a function of F_i'. In this figure Rs is given by Eq. (4) and using Eq. (3) the force-voltage transfer function can be written as

$$V = \frac{F_i' s\phi C_0 R_{num}(1 - z^{-m_0}) \cdot f^*}{Z_{eqnum}}, \tag{16}$$

where

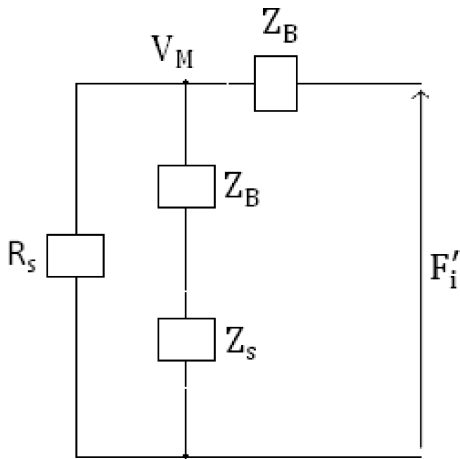$$f^* = [Z_c Z_{sden}(1 - z^{m_0}) + Z_{snum}(1 + z^{-m_0})].$$

Fig. 4. Simplified circuit used for the calculation of V_M (Fig. 2) in terms of the force face of the piezoelectric element F_i'.

For Eqs. (9), (12), (15), and (16) to be fully represented in terms of discrete time, a discrete approximation to the Laplace variables has to be incorporated into this expression. The transfer equation can be solved as a recursive digital filter and these equations can be easily implemented using polynomial algebra routines.

3. Results

The simulation is applied using typical transducer data constructed with a lead zirconate titanate (PZT-5A) piezoelectric element (BERLINCOURT *et al.*, 1964) with a different quarter-wave length matching layers. The transmitter response is obtained for a 10-mm-diameter pulse-echo transducer of 5 MHz center frequency and radiating into water medium. The transducer diameter (10 mm) is much greater than its thickness (0.435 mm). As a result, it fulfills the requirement of a 1D transducer model. Figure 5 shows the expected waveform of an air backed transducer when the device acts as a receiver with no matching layer. Once the impulse response is obtained, a fast Fourier transform is performed on the data. Figure 6 shows the pulse-echo transducer frequency response. From this figure, it can be seen that the backing layer of air yield −3 dB bandwidth of 0.31 of the central frequency. Let us now examine changes in the performance of transducer with one, two and three quarter wavelength matching layers. Varying each of the matching layers of practical
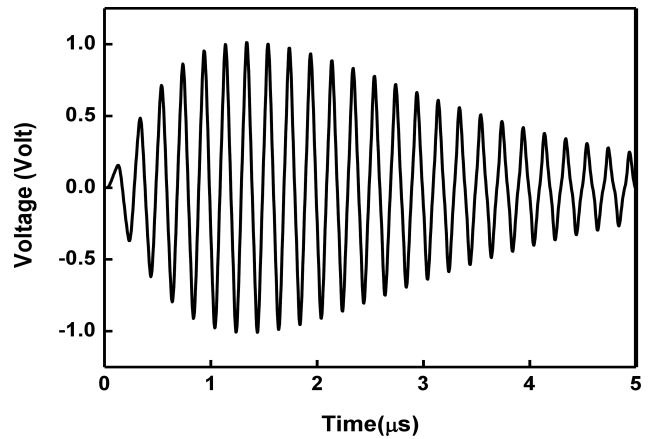

Fig. 5. The pulse-echo transducer response with no matching layer operating into water load and air backing.
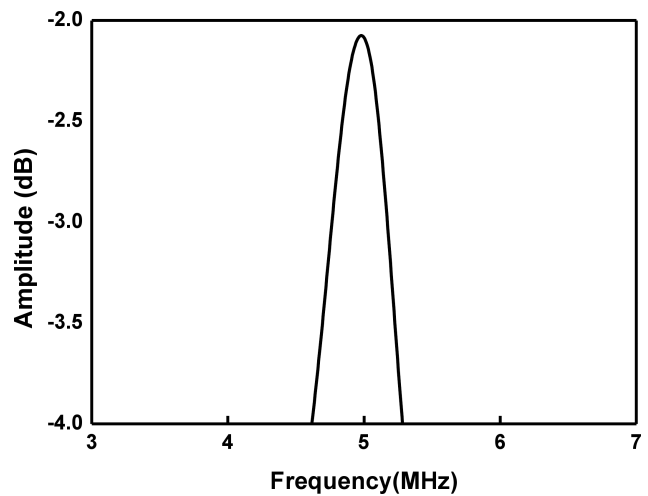

Fig. 6. Pulse-echo transducer frequency response for Fig. 5.

materials enables us to determine the optimum combination of layers/materials that gives a wide bandwidth. The optimized impedance formula is given by (GOLL et al., 1975):

$$\ln\left[\frac{Z_{n+1}}{Z_n}\right] = 2^{-N}\frac{N!}{(N-n)!n!}\ln\left[\frac{Z_{RF}}{Z_0}\right], \qquad (17)$$

where Z_n is the n-matching layer impedance, N is the total number of matching layers, Z_0 is the acoustic impedance of the piezoelectric material, and Z_{RF} is the acoustic impedance of the load medium (water). The sensitivity was defined as the maximum height of the received pulse, given in terms of volts. Using the matching layer of practical material values reported in Table 1, the sensitivity and bandwidth for the single quarter-wave length matching layer was reported in Fig. 7. It is clear that the sensitivity is maximized and duration pulse is minimized when the matching layer is Glassbeads (SOUQUET et al., 1979). Table 2 shows the optimum parameters for materials used for one, two, and three matching layers. Figure 8 shows the expected waveform at the transducer terminals when the device acts as a receiver with one, two, and three matching layers of air backed transducer. Figure 9 shows the pulse-echo frequency responses for zero, one, two, and three matching layers. It is clear from this figure that the matching layers of one, two, and three layers yield – 3 dB bandwidths of 0.54, 1.1 and 1.4 of the center
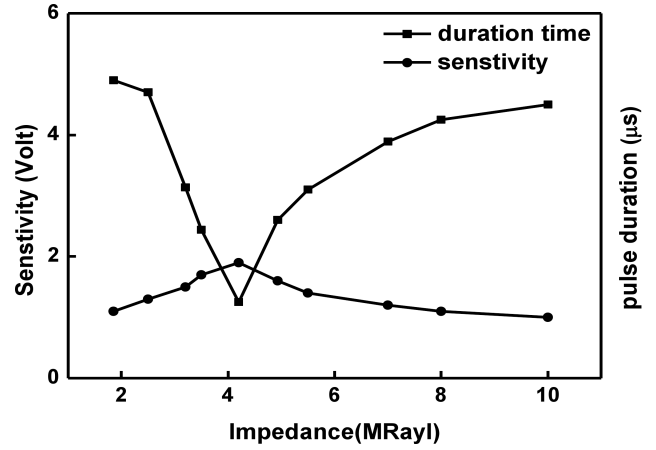

Fig. 7. Dependence of sensitivity and duration pulse on the first matching layer.

frequency, respectively and the results are consistent with Eq. (17).

For bonding ceramics, it is common practice to use epoxy resins, such as Araldite, which has very low impedance compared with ceramics. Therefore, if the bond is insufficiently thin, there will be an impedance mismatch at the ceramic interface, causing degradation of transducer performance. SILK et al. (1983) showed that an Araldite bond between ceramics and a high impedance backing must have a thickness of less than

Table 1. Variety of single matching layer with pulse duration and sensitivity.

Material for quarter wave length	Sensitivity [Volt]	Pulse duration [μs]	Impedance (Z) [Kg/m^2.s]$\times 10^6$
Mathylplaten	1.85	4.9	1.1
Polystyrene	2.5	4.7	1.3
Polymethylmeth-acrylate	3.2	3.14	1.5
Glassbeads and Epoxy	4.0	2.44	1.7
Glassbeads-Epoxy [16]	**4.2**	**1.25**	**1.9**
Melopas	4.93	2.6	1.6
AL-Epoxy	5.5	3.1	1.4
Tungsten-araldite	7.0	3.89	1.2
Glass arsenic trisulphide	8.0	4.25	1.1
Tungsten-Epoxy	10.0	4.5	1.0

Table 2. The optimum value of single, two and three matching layers as a function of sensitivity and duration pulse.

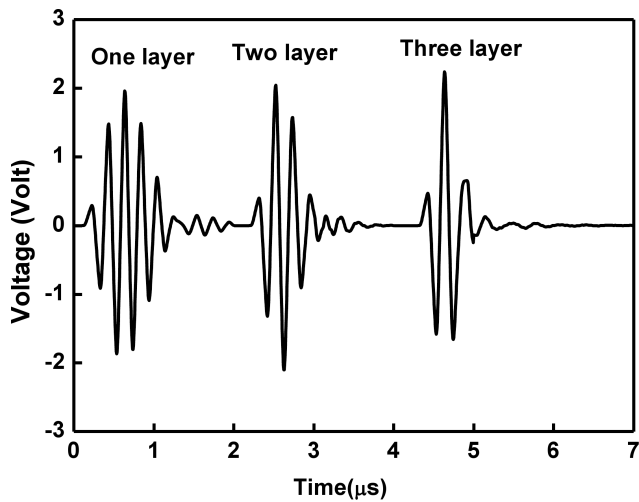| Material for quarter wavelength		Impedance (Z) [Kg/m^2.s]$\times 10^6$	Acoustic velocity [m/s]	Pulse duration [μs]	Sensitivity [Volt]
One matching layer	Glassbeads and Epoxy	4.2	2300	1.25	1.9
Two matching layers	Glass arsenic trisulphide	8.0	3000	0.8	2.1
	Polystyrene	2.5	2550		
Three matching layers	Glass	14.6	5943	0.7	2.4
	Glassbeads and Epoxy	4.2	1900		
	Methyl-platen	1.85	970		

Fig. 8. The pulse-echo transducer responses with single, two and three matching layers operating into water load. These three curves are shifted to emphasize the effect on duration of the signal.
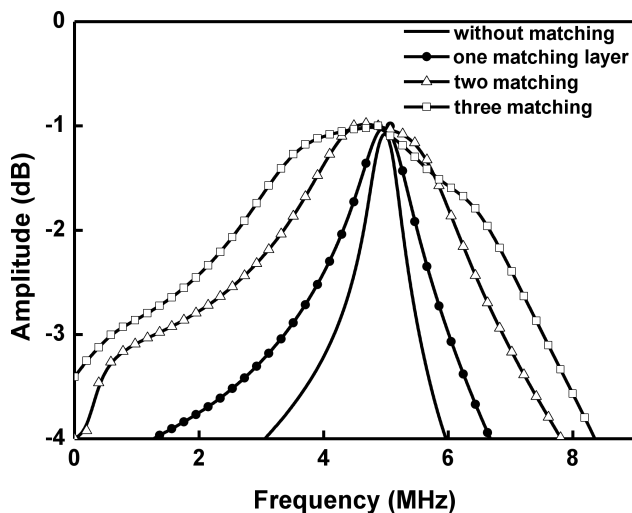

Fig. 9. Amplitude frequency spectrum for one, two and three matching layers and without matching layer.
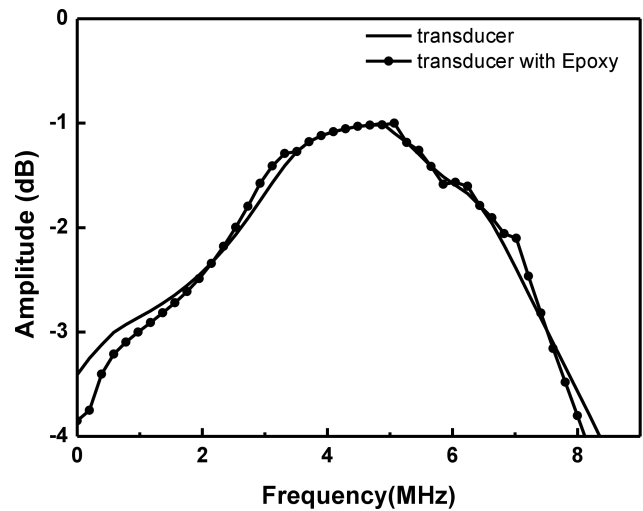

Fig. 10. Amplitude frequency spectrum of three matching layers with bondlines and no bondlines.

(ALI, 2000). Figure 11 shows the frequency response of the three matching layers with back matching layer of copper. The -3 dB bandwidth increases from 1.4 to 1.48.
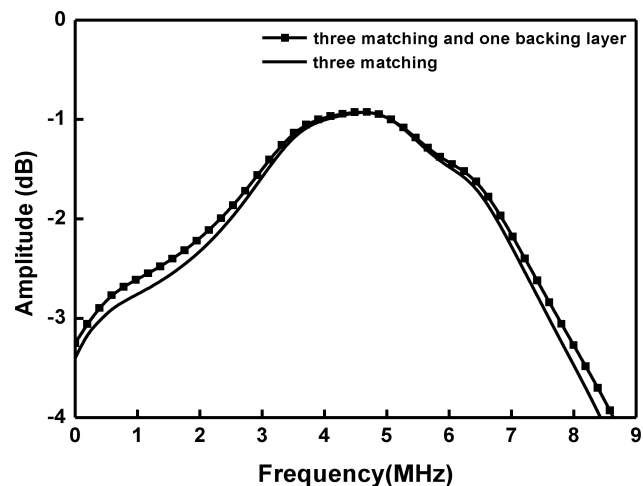

Fig. 11. Effect of backing one layer of copper as backing with three front matching layers.

MULHOLLAND *et al.* (2008) recorded impulse frequency response for 1 MHz probe with four matching layers as shown in Table 3. The matching layer

Table 3. Materials properties for the experimental multi-layer matching scheme (MULHOLLAND *et al.*, 2008).

Material for four matching quarter wavelength	Impedance [Kg/m^2.s]$\times 10^6$	Acoustic velocity [m/s]
Soda Lime Glass	14.6	5943
Vitreous Carbon	6.7	4723
BaSO$_4$ filled epoxy	2.9	2592
Epoxy	2.1	1784

$\lambda/200$ to avoid adverse effects. At 5 MHz this corresponds to 10 μm which can be used as an indication of the required bond thickness. Figure 10 shows the frequency response for three matching layers with 10 μm bond-lines as compared to that of an idealized device with no bond materials. It can be seen that the bonding material thickness has very little effect on the frequency response. The -3 dB bandwidth drops from 1.4 to 1.3. The backing layer is required when the performance of the front matching layers is nonideal, which is often the case because of limitations in available materials. Resonance is formed by the reflection from front and back face. If reflections from the front face are zero as a result of the use of an ideal front matching layer, performance is improved because resonance cannot be formed solely from reflections from the back boundary
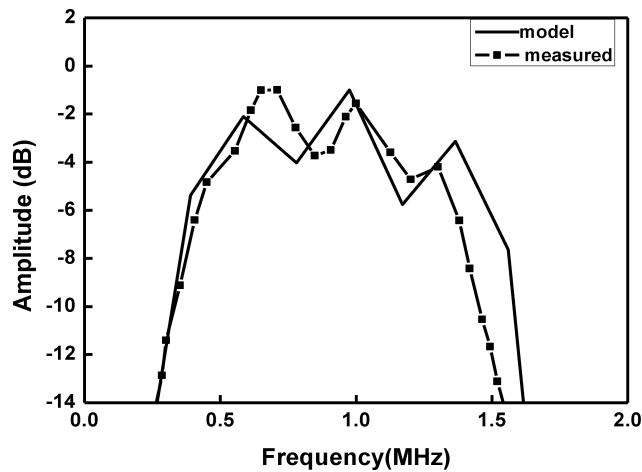
Fig. 12. Experimental transducer frequency response is compared with the proposed model.
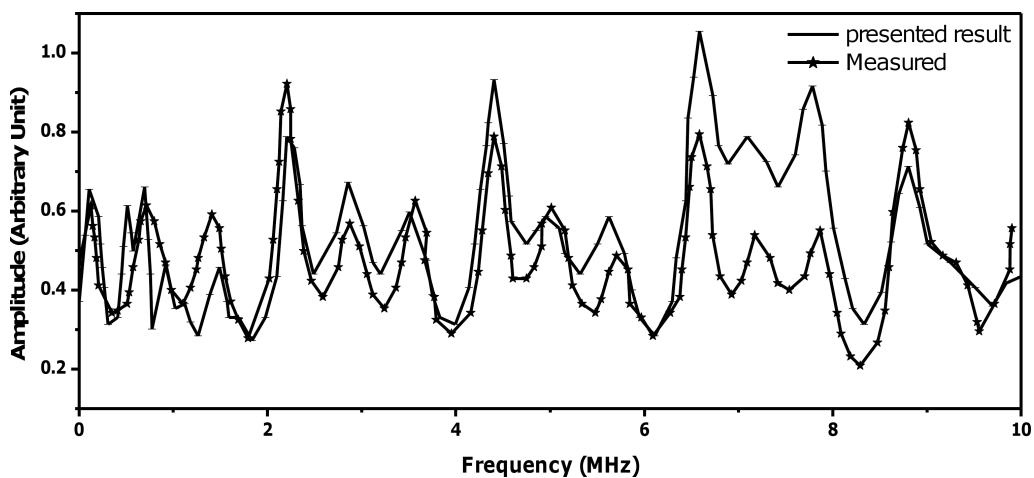

Fig. 13. Comparison of the measured and the presented model through transmission impulse response for the four matching layers.

was then attached to the piezoelectric element and attached to a backing block material with an acoustic impedance of 8 MRayls. The pulse-echo impulse response of the transducer was measured in a water tank using a Panametrics 5052PR pulser-receiver to excite the transducer. The echo from a glass block was recorded using a digitizing oscilloscope and was converted to the frequency domain using the FFT. Figure 12 shows the experimental transducer pulse-echo impulse response in the frequency domain (MULHOLLAND *et al.*, 2008) together with presenting modelled response. Figure 13 shows the comparison of the experimental (MULHOLLAND *et al.*, 2008) and the presented model for four matching layers. It is clear that the predicted result is in good agreement with the published experimental data. It is clear from all of these results that calculation using the transducer equivalent circuit proposed in this paper yields an accurate analysis in the design of sensitive short response of air backed transducer.

4. Conclusions

A discrete time model of the thickness mode piezoelectric transducer was used to predict the influence of mechanical layers and intermediate bond lines on the impulse response. The model was obtained from the analysis of the electrical equivalent circuit of a piezoelectric device. The model was implemented directly in the time domain. The optimum acoustic characteristics of the matching layers were determined by defining a compromise between the sensitivity and the pulse duration of impulse response. The effects of bonding layers are smaller so that they do not change the resonance peak significantly. The calculated results show that the -3 dB air backed transducer bandwidth can be improved significantly by using quarter matching layers. The results presented in this paper show that the optimized model predicts measurement results of the received echo waveform and its frequency spectrum. The method has the advantage that the time

signal for an optimum set of matching layers of practical materials can be predicted immediately.

References

1. ALI M.G.S., ELSAYED N.Z., ABDEL FATTAH A.M., ALI GHARIEB A. (2012), *Loss mechanisms in piezoceramic materials*, J. Comput. Electron, **11**, 196–202.

2. ALI M.G.S. (2000), *Analysis of Broadband Piezoelectric Transducers by Discrete Time Model*, Egypt. J. Sol., **23**, 2, 287–295.

3. ALI M.G.S. (1999), *Discrete time model of acoustic waves transmitted through layers*, Journal of Sound and Vibration, **224**, 2, 349–357.

4. BEERMAN H.P. (1981), *Optimizing matching layers for three-section broadband piezoelectric PZT-5A transducer operating into water*, IEEE Trans. Sonics Ultrason., **SU28**, 1, 52–53.

5. BERLINCOURT D.A., CURRAN D.R., JAFFE H. (1964), *Piezoelectric and piezomagnetic materials and their function in transducers*, Physical Acoustics IA, Mason W.P. [Ed.], Academic, New York.

6. DESILETS C.S., FRASER J.D., KINO S., GORDON S. (1978), *The design of efficient broad-band piezoelectric transducers*, Sonics and Ultrasonics, IEEE Transactions, **25**, 3, 115–125.

7. ESTANBOULI Y., HAYWARD G., RAMADAS S.N., BARBENEL J.C. (2006), *A block diagram model of the thickness mode piezoelectric transducer containing dual oppositely polarized piezoelectric Zones*, IEEE Transactions on Ultrasonics, Ferroelectrics, and Frequency Control, **53**, 5, 1028–1036.

8. GOLL J.H., AULD B.A. (1975), *Multilayer Impedance Matching Schemes for Broad banding of Water Loaded Piezoelectric Transducers and High Q Electric Resonators*, IEEE Transactions on Sonics and Ultrasonics, **22**, 1, 52–53.

9. JURY E.I. (1964), *Theory and application of the z-transform method*, Wiley, New York.

10. KAZYS R., DEMCENKO A., ZUKAUSKAS E., MAZEIKA L. (2006), *Air-coupled ultrasonic investigation of multi-layered composite materials*, Ultrasonics, **44**,1, 819–822.

11. KAZYS R. (1978), *Structural optimization methods of electroacoustic measuring circuits with piezoelectric transducers*, Ultragarsas, **10**, 29–42.

12. KAZYS R., LUKOSEVICIUS A. (1977), *Optimization of the piezoelectric transducer response by means of electrical correcting circuits*, Ultrasonics, **15**, 111–116.

13. KONOVALOV S.I. (2002), *The effect of the matching layer thickness on the duration of pulses generated by a transducer*, Acoustical Physics, **48**, 5, 618–619.

14. LEE H., CHOI S., MOON W. (2010), *A micro-machined piezoelectric flexural-mode hydrophone with air backing: benefit of air backing for enhancing sensitivity*, J. Acoust. Soc. Am., **128**, 3, 1033–1044.

15. LEWIS G.K. (1980), *A Matrix Technique for Analyzing the Performance of Multilayered Front Matched and Backed Piezoelectric Ceramic Transducers*, Acoustical Imaging, **8**, 395–416.

16. MULHOLLAND A.J., RAMADAS N., O'LEARY R.L., PARR A.C.S., HAYWARD G., TROGE A., PETHRICK R.A. (2008), *Enhancing the performance of piezoelectric ultrasound transducers by the use of multiple matching layers*, Journal of Applied Mathematics, **73**, 6, 936–949.

17. OPPENHEIM A.V., SCHAFER R.W. (1975), *Digital signal processing*, Prentice-Hall, New Jersey.

18. PERSSON H.W., HERTZ C.H. (1985), *Acoustic impedance matching of medical ultrasound transducer*, Ultrasonics, **23**, 2, 83–89.

19. SHERRITY S., WIEDERICK H.D., MUKHERJEE B.K., SAYER M. (1997), *An accurate equivalent circuit for the unloaded piezoelectric vibrator in the thickness mode*, Journal of Physics D: Applied Physics, **30**, 16, 2354–2363.

20. SILK M.G. (1983), *Predictions of the effect of some constructional variables on the performance of ultrasonic transducers*, Ultrasonics, **21**, 27–33.

21. SHUNG K.K., CANNATA J.M., ZHOU Q.F. (2007), *Piezoelectric materials for high frequency medical imaging applications: A review*, Journal of Electro Ceramics, **19**, 141–147.

22. SOUQUET J., DEFRANOULD P., DESBOIS J. (1979), *Design of low-loss wide-band ultrasonic transducers for noninvasive medical application*, IEEE Pans. Son. Ultrason., **SU-26**, 75–81.

23. TODA M., THOMPSON M. (2010), *Novel multi-layer polymer-metal structures for use in ultrasonic transducer impedance matching and backing absorber applications*, IEEE Trans. Ultrason. Ferroelectric. Freq. Control, **57**, 12, 2818–2827.

24. TODA M., THOMPSON M. (2012), *Detailed Investigations of Polymer/Metal Multilayer Matching Layer and Backing Absorber Structures for Wideband Ultrasonic Transducers*, IEEE Transactions on Ultrasonics, Ferroelectrics, and Frequency Control, **59**, 2, 231–242.

25. YAACOB M.I.H., ARSHAD M.R., MANAF A.ABD. (2011), *Modeling of circular piezoelectric micro ultrasonic transducer using $CuAl_{10}Ni_5Fe_4$ on ZnO film for sonar applications*, Acoustical Physics, **57**, 2, 151–158.

26. YEONGCHIN CHEN (2010), *Acoustical transmission line model for ultrasonic transducers for wide-bandwidth application*, Acta Mechanica Solida Sinica, **23**, 2, 124–134.